

Published in final edited form as:

*Trends Pharmacol Sci.* 2011 November ; 32(11): 637–643. doi:10.1016/j.tips.2011.08.001.

## GPCR agonist binding revealed by modeling and crystallography

Vsevolod Katritch<sup>^</sup> and Ruben Abagyan

Skaggs School of Pharmacy and Pharmaceutical Sciences and San Diego Supercomputer Center, University of California, San Diego, La Jolla, CA 92093, USA

### Abstract

While structural coverage of the G-protein coupled receptor (GPCR) family steadily improves, high plasticity of these membrane proteins poses additional challenges for crystallographic studies of their complexes with different classes of ligands, especially agonists. Ability to computationally predict binding of natural and clinically relevant agonists and corresponding changes in the receptor pocket, starting from inactive GPCR structures, is therefore of great interest for understanding GPCR biology and drug action. Comparison of published in 2009 and 2010 computational models with recently determined agonist-bound structures of  $\beta$ -adrenergic and adenosine  $A_{2A}$  receptors reveals high accuracy of the predicted agonist binding poses (0.8 Å and 1.7 Å respectively) and receptor interactions. In the case of the  $\beta_2$ AR, energy-based models with limited backbone flexibility also allowed characterization of side chain rotations and a finite backbone shift in the pocket region as determinants of full, partial or inverse agonism. Development of accurate models of agonist binding for other GPCRs will be instrumental for functional and pharmacological studies, complementing biochemical and crystallographic techniques.

### G protein-coupled receptors

As the key players in recognition of extracellular signals, G protein-coupled receptors (GPCRs) represent the largest (>800) and most important superfamily of clinical targets in disorders of neural, immune, cardiovascular, endocrine systems and cancer [1–3]. GPCRs can be activated by endogenous or synthetic agonists, inhibited by antagonists and inverse agonists, or affected by allosteric modulators [4], and each of these classes of ligands is therapeutically relevant. The crystal structures of  $\beta$ -adrenergic ( $\beta_2$ AR and  $\beta_1$ AR)[5–8], adenosine  $A_{2A}$  ( $A_{2A}$ AR)[9], chemokine CXCR4 [10], dopamine D3 (D3R) [11], and most recently histamine H1 (H1R)[12] receptors in complex with stabilizing antagonists provide a long sought 3D structural framework for studies of GPCR function and future drug discovery efforts ([13, 14]). Over the last few years, applicability of docking and virtual ligand screening (VLS) technologies to GPCR crystal structures [15–18] has been validated by co-crystallization of some of these ligands [8] and prospective identifications of novel  $\beta_2$ AR and  $A_{2A}$ AR antagonist chemotypes [19–23]. Similar VLS studies are likely under way

© 2011 Elsevier Ltd. All rights reserved.

Corresponding authors: Katritch, V. (katritch@scripps.edu) and Abagyan, R. (rabagyan@ucsd.edu).

<sup>^</sup>Current address: Department of Molecular Biology, The Scripps Research Institute, 10550 North Torrey Pines Rd., GAC-1200, La Jolla, CA 92037, USA

**Publisher's Disclaimer:** This is a PDF file of an unedited manuscript that has been accepted for publication. As a service to our customers we are providing this early version of the manuscript. The manuscript will undergo copyediting, typesetting, and review of the resulting proof before it is published in its final citable form. Please note that during the production process errors may be discovered which could affect the content, and all legal disclaimers that apply to the journal pertain.

for other therapeutically relevant GPCRs, whose structures have appeared over the last year [10–12].

At the same time, intrinsic plasticity of GPCRs was thought to be a major obstacle for using inactive state receptor structures for analysis of agonist binding (e.g. see [24]). Indeed, plasticity is a part of GPCR function in signal transduction across the cellular membrane, with large scale changes experimentally found in the intracellular G-protein interaction site [25, 26]. Quite significant rearrangements were expected in the ligand binding pocket as well, where rotations of the transmembrane 6 (TM6) and TM7 helices, and aromatic side chain rotamer switches (e.g. the W6.48 “toggle switch”) were proposed [27]. The complexity and magnitude of the proposed changes, and discrepancies between ligand binding poses implied low accuracy of those early models, based on distant homology with rhodopsin.

The new platform for ligand binding modeling established in 2007 by high resolution crystal structures of the inactive  $\beta_2$ AR-carazolol complex [5], suggested that agonist-dependent changes in the pocket could be rather limited and specific, yet predictable [17, 28]. The structure-based models with backbone flexibility also suggested specific triggers of the receptor activation, explaining the structural basis of full, partial and inverse agonism in the  $\beta_2$ AR [17]. Agonist binding to the  $A_{2A}$ AR was also modeled [18, 29] based on its crystal structure in inactive form [9], though in this case flexibility was limited to the pocket side chains. Here we compare these blindly predicted models with the recently determined crystal structures of agonist-bound complexes of  $\beta_2$ AR [30, 31],  $\beta_1$ AR [32], and  $A_{2A}$ AR [33, 34]. The results show utility of the structure-based conformational modeling in analysis of ligand-dependent functional plasticity in GPCR binding pocket, as well as in providing a 3D framework for rational drug discovery.

## Details of $\beta_2$ AR agonist binding revealed by modeling and crystallography

Early biochemical and mutagenesis studies of the  $\beta_2$ AR have established two major anchor interactions for full agonists, in which common amino groups form a salt bridge to Asp113<sup>3.32</sup> carboxyl [35], while the polar groups of catechol or similar moiety interact with serine side chains in TM5 [36, 37]. Other details of agonist interactions and agonist-induced changes in the  $\beta_2$ AR pocket were also proposed based on modeling interpretation of experimental data, such as (i) rotamer switch in W6.48 and other aromatic residues (“rotamer toggle switch”) [38], (ii) “up” orientation and polar interaction with Asn293<sup>6.55</sup> for  $\beta$ -OH group in agonists [39], (iii) direct interaction of the catechol group with Ser204<sup>5.43</sup> in TM5; all of these specific changes require large rearrangements of TM6 and TM7 backbone in the binding pocket (e.g. reviewed in [27] and [40]).

Availability of the high-resolution inactive  $\beta_2$ AR-carazolol structure in 2007 (PDB:2rh1)[5] provided a new structural platform and new wave of interest for deciphering mechanisms of agonist binding and activation in GPCRs (e.g. reviewed in [41]). Some of the new models published as recently as 2011 reproduced the early concepts, including rotamer toggle switch and  $\beta$ -OH contact with Asn293<sup>6.55</sup> [42, 43], and/or introduced other large scale motions in the pockets such as 60° axial rotation of TM5 [44]).

Conversely, other docking and modeling studies supported much smaller changes in the inactive crystal structure of the  $\beta_2$ AR upon agonist binding [45]. Thus, the initial agonist-induced fit can be modeled by changing only rotameric states of serine side chains in TM5 [16, 17, 28], though these changes were thought to represent low-affinity binding mode of agonists. More comprehensive analysis of  $\beta_2$ AR ligand binding in flexible  $\beta_2$ AR models performed in 2008 also identified a finite  $\sim 2$  Å inward shift of TM5 as a requirement for optimal (“high-affinity”) binding of full agonists [17]. This study used energy-based

docking [46, 47] in an atomistic model of the  $\beta_2$ AR with fully flexible side chains and limited backbone flexibility in TM5 domain. A physics-based energy function and highly efficient biased probability monte carlo (BPMP) procedure [48] in internal coordinates [49] allowed global convergence of the conformational sampling. Importantly, the procedure did not use ligand-receptor restraints, allowing the model to naturally sample possible ligand-receptor contacts. Similar TM5 shift was also obtained later by Vilar *et al.* [50] in a 2011 study that used induced fit docking and molecular dynamics with backbone flexibility expanded to all TM helices. While supporting the two anchor interactions for full agonists (with Asp113<sup>3,32</sup> and TM5 serines), modeling results in ref. [16, 17, 50] questioned the other important details of agonist binding and proposed alternative interpretations of experimental data (Figure 1). Thus, the  $\beta$ -OH moiety of the ethanolamine “tail” of agonists was found consistently docked into the same anchor site between Asp113<sup>3,32</sup> and Asn312<sup>7,39</sup> as carazolol and other inverse agonists and antagonists [8]; the role of Asn293<sup>6,55</sup> in agonist stereo selectivity [39] was explained by interactions with catechol ring instead of direct contact with  $\beta$ -OH. Also, optimal conformations of agonists did not require rotamer “toggle switch” [38] in W286<sup>6,48</sup> or other aromatic residues in the pocket, suggesting similar contacts of the ligand aromatic “core” across all classes of high-affinity  $\beta_2$ AR ligands.

At the same time, the key difference between the binding of inverse agonists and full agonists was explained in these models by a finite inward shift and positional restraint of the TM5 extracellular portion. The TM5 shift in the model occurred as a consequence of relatively high conformational freedom in this domain and strong hydrogen bonding between the ligand catechol “head” and reoriented Ser203<sup>5,42</sup> and Ser207<sup>5,46</sup> side chains. Unlike the other two serines in TM5, the Ser204<sup>5,43</sup> side chain did not make contact with catecholamine agonists, while its role in binding and activation was explained by polar interaction with Asn293<sup>6,55</sup>, which helped to stabilize inward shift of TM5 helix (Figure 1). The resulting pocket contraction between helices TM5 and TM3/TM7 allowed optimal engagement of both agonist ethanolamine tail and polar groups on the aromatic system with anchor sites of polar interactions in the model, characteristic for the high-affinity binding state of  $\beta_2$ AR -agonist complexes. Based on this modeling and existing structure-activity relationship (SAR) and mutagenic data [36, 37, 51–55], the magnitude of the ligand-induced shift in TM5 was predicted to be one of the key determinants that distinguished between full and partial activation of the  $\beta_2$ AR, whereas blocking of the inward TM5 movement provided an explanation for reduction of basal activity by inverse agonists.

We were very pleased to find these modeling predictions to be largely validated by the recently published structures of  $\beta_2$ AR and  $\beta_1$ AR complexes with agonists [30, 32]. Both  $\beta_2$ AR and  $\beta_1$ AR co-crystals show high precision of our binding pocket models and a number of non-trivial details of ligand polar interactions with TM5 and TM6 side chains (Figure 2). Accuracy of the predictions for agonist binding poses (Root Mean Square Deviation (Rmsd) = 0.8 Å and 0.5 Å for two full agonist models) and contact side chains (Rmsd = 1.1 Å and 0.9 Å respectively) is comparable with those expected for crystal structures in the Protein Databank (PDB) [56]. Moreover, the crystal structure of activated state agonist- $\beta_2$ AR complex [30] (PDB code 3P0Q) reveals contraction of the pocket via 2.1 Å inward shift of TM5 top part above conserved Pro211<sup>5,50</sup>, similar to the 2.0 Å TM5 shift in our blind predictions (compare Figure 4 in [17] and Figure 4a in [30]). While movements in TM3 (Asp113<sup>3,32</sup>) and TM7 (Asn312<sup>7,3</sup>) also contribute to this compaction, both do not exceed 0.4 Å in the activated  $\beta_2$ AR structure [30].

Note that our flexible docking study [17] did not attempt to model the downstream activation-related changes in the receptor intracellular half, which for the modeling purposes were considered as decoupled from immediate ligand-induced changes in the pocket. Such

decoupling is not only a practical trick to focus modeling on the binding pocket itself, but it may partially reflect crystallographic behavior in some GPCR-agonist systems [32], as discussed below.

## Adenosine A<sub>2A</sub> agonist binding predictions

Adenosine A<sub>2A</sub> receptor (A<sub>2A</sub>AR) modeling studies [18, 29] provide another example of successful modeling of agonist binding based on an inactive GPCR structure [9]. Our study [18] combined mutagenetic experiments with theoretical predictions, where the agonist NECA (5'-N-ethylcarboxamido adenosine) and its C2 substitute CGS21680 were docked into the crystal structure with subsequent refinement of the pocket side chains. As in the case of the  $\beta_2$ AR, the predicted A<sub>2A</sub>AR agonist docking poses suggested some interactions that are common for agonist and antagonist binding, including aromatic ring and exocyclic amine core contacts, as well as distinct new interactions specific for ribose moiety of agonists. Although initial rigid docking gave an ambiguous binding pose with suboptimal polar interactions, the energy-based ligand-guided refinement of the binding pocket made possible selection of one optimal pose of the ribose ring shown in Figure 3. The refinement also made possible prediction of the binding energy changes for several mutations in the pocket, which turned out to be in qualitative agreement with experimental assays. Similar binding poses and orientation of the ribose ring were predicted independently by Ivanov *et al.* for NECA and endogenous ligand adenosine [29].

The first agonist-bound A<sub>2A</sub>AR crystal structures have been determined very recently, thanks to identification of a conformationally selective agonist UK-432097 in one case [33] and extensive mutagenetic screening in the other [34], both helping to stabilize A<sub>2A</sub>AR in activated form. Despite the differences in ligands and receptor stabilization technologies, the position and receptor contacts for the common adenosine scaffold for UK-432097 (PDB: 3QAK), NECA (PDB:2YDO) and adenosine (2YDV) in these three structures is essentially identical (Rmsd < 0.5 Å). Comparison of this common scaffold with the A<sub>2A</sub>AR-NECA models shows close similarity of the predicted poses overall and in the ribose ring specifically, with Rmsd = 1.7 Å for [18], 1.9 for [29], and 0.9 Å between the two independent NECA models in these studies. Models in both studies predicted all major polar interactions of the ribose rings, including H-bonds with His278<sup>7,43</sup>, Ser277<sup>7,42</sup> and Thr88<sup>3,36</sup>, though the latter interaction had apparently suboptimal 4.5–4.7 Å donor-acceptor distance [33].

The difference in agonist position between the crystal structure of the activated A<sub>2A</sub>AR and the models can largely be explained by a systematic ligand shift by about 1.4–1.5 Å. Unlike  $\beta_2$ AR-agonist modeling described above [17], the preliminary modeling of A<sub>2A</sub>AR-agonist binding [18, 29] did not attempt to include backbone changes in conformational refinement of the complex. As is now apparent from the crystal structures, more accurate positioning of the ligand and formation of optimal H-bond with Thr88<sup>3,36</sup> would be impossible without certain changes in the receptor. These changes involve shifting of the Trp246<sup>6,48</sup> side chain that allow agonists to settle into position slightly deeper in the binding pocket, and also the upward shift of TM3 helix along its axis that brings T88<sup>3,36</sup> hydroxyl into optimal contact with the amino substitute of the ribose ring.

## What can we learn about activation mechanisms from modeling?

As illustrated by the  $\beta_2$ AR [16, 17, 28, 50] and A<sub>2A</sub>AR [18, 29] examples, conformational modeling based on inactive GPCR structures and available biochemical data can predict agonist binding poses with accuracies in some cases comparable to crystal structures. In both receptors, initial docking of agonists into inactive receptor conformations was accommodated by only minor changes in the pocket side chains; such models may

correspond to a low affinity ligand binding state of the receptor. In the  $\beta_2$ AR case [17, 50], modeling was also successful in predicting contraction of the pocket via movement of TM5 helix (1–2 Å), which corresponds to high affinity binding state, very similar to those found later in the activated crystal structure of the  $\beta_2$ AR [30]. Of course, accuracy of the conformational modeling depends on the range of agonist-induced movements in the pocket, especially in the protein backbone. Although both currently available structure-validated examples support a limited range of agonist-induced pocket changes and predictability of agonist binding, further theoretical and structural studies may be required to test this hypothesis for other GPCR subfamilies.

Whereas the above modeling studies focused on ligand binding and changes the extracellular pocket, they did not attempt to model coupling of the ligand induced changes with activation-related downstream rearrangements in G-protein binding site. Such downstream changes, including dynamics of ionic lock and other “microswitches” have been the subject of several other modeling studies (e.g. [41, 57]). The nature of the downstream changes has been also revealed by active-like ligand-free opsin structures [26, 58] and all-trans retinal Rhodopsin [59], and most recently by structures of activated  $A_{2A}$ AR [33] and  $\beta_2$ AR in complex with G-protein [60] or its surrogate [30]. The consensus changes for all three activation models on the intracellular side include inward shift of TM7 and a concerted movement of TM5 and TM6, where the latter is swinging outward and opens a crevice for insertion of  $G\alpha$  terminus. Interestingly, soft coupling between (1) initial ligand binding, (2) small extracellular and (3) large downstream changes is not only a convenient approximation useful in modeling of agonist receptor interactions described here [17, 18, 28], but also seems to reflect the allosteric nature of the activation mechanism in GPCRs [61]. Thus, recent crystal structures captured a covalently-bound full agonist FAUC50 in the  $\beta_2$ AR conformation that is indistinguishable from inactive one [31], suggesting decoupling of stages 1 and 2. Another structure, that of thermostabilized  $\beta_1$ AR complex with full agonist isoproterenol, shows a receptor with at least partial changes in the binding pocket (1 Å shift of TM5), but lacking any downstream changes in the intracellular part, showing partial decoupling of stages 2 and 3 [32].

Besides these general trends, both modeling and crystallography suggest that immediate triggers of the agonist dependent activation can vary a lot between GPCRs, which can also be expected from diversity of GPCR ligands and binding pockets. Thus, observed in the  $\beta_2$ AR direct polar interactions of TM5 serines with agonists and corresponding movements in TM5 helix [31], were not found in the  $A_{2A}$ AR, where pocket contraction results mostly from agonist-mediated shift of TM7 towards TM3. Moreover, even within adrenergic family, TM5 movement is unlikely to play such an important role, as many of these GPCRs lack polar groups in the corresponding positions in TM5 or TM7 (e.g. D3R [11]). Another type of trigger involves ligand steric “push” on specific side chains in the pocket, as a result of ligand adjusting its position to fully optimize interactions in the pocket. Comparison of inactive and activated  $A_{2A}$ AR, for example [33], shows that the ribose ring of agonists cannot optimally fit in the pocket without about 2 Å movement of the conserved Trp6.48 side chain in the “cWXP” motif. In contrast,  $\beta_2$ AR agonists do not make direct contact with the W6.48 side chain, and its smaller movement may be indirectly promoted by ligand TM5 shift via side chain changes in Ile121<sup>3.40</sup> and Phe282<sup>6.44</sup> as suggested in ref.[30]. Note that the movements of Trp6.48 observed in all crystal structures, including fully activated  $\beta_2$ AR- $G\alpha\beta\gamma$  complex [60] do not actually involve “rotamer toggle switch” in this residue [38]. Instead, the Trp6.48 side chain moves together with the protein backbone, promoting partial unwinding of TM6 in the Proline induced kink, and corresponding swing of the TM6 intracellular tip.



Some other movements of TM helices may depend on ligand choice for both active and inactive crystal forms, reflecting conformational (and potentially functional [62]) selectivity. Such an example can be found in the A<sub>2A</sub>AR complex with UK-432097 agonist, where the bulky C2 and N6 substituents of this compound apparently push on extracellular loop 3 (ECL3) and the top of the TM7 helix, promoting a seesaw movement of TM7. In some cases such consequences of ligand-specific motions may be possible to predict computationally, giving insight into conformational and functional selectivity of ligands. In other cases, exemplified by concerted movement in TM5 and TM6 recently described in detail for the adrenergic receptor [30], molecular mechanisms connecting extracellular and intracellular changes can be surprisingly complex and less predictable. Moreover, better understanding of such details of functional selectivity may require further structural and biochemical studies of GPCR complexes with G-proteins [60] and other downstream effectors.

## Applications to GPCR drug discovery

As the pace of GPCR structure determination improves, there are several highly encouraging examples showing utility of the crystal structures in discovery of new high affinity compounds as potential drug leads [20, 21]. However, it is not clear if a standard structure-based drug discovery paradigm, which requires routine co-crystallization of receptors with novel lead molecules, would work for GPCRs. Because of their intrinsic flexibility, GPCRs are preferably crystallized with selected high-affinity stabilizing compounds, while crystallization with suboptimal leads requires elaborate point mutation technologies to achieve sufficient stability [32, 34, 63]. Moreover, even within the same subfamily, some GPCR subtypes will be less amenable to crystallization, leaving desirable targets without crystal structures.

Conformational modeling is perfectly positioned to fill these significant gaps in structural knowledge. As the computational studies here suggest, energy-based conformational modeling can accurately predict binding poses and certain levels of ligand induced fit in the binding pocket, including small shifts in protein backbone. Such refined models of GPCR-lead complexes will be of great value for rationalizing existing SAR data and can direct structure-guided design of substitutions for lead optimization.

Another potential application of GPCR binding pocket models is virtual ligand screening (VLS) for novel chemotypes. This tool is relevant for many GPCR targets, given rather limited chemical space explored so far by traditional drug discovery methods like HTS and ligand based scaffold hopping. We show that models optimized for binding of a specific ligand class, e.g. agonist-optimized models, can be highly selective for this class in a large scale virtual screening (VLS) benchmark [16]. Recently, this approach was developed into an automated iterative ligand guided receptor optimization algorithm (LiBERO)[64, 65] that generates an optimal VLS model conformation based on a defined set of known ligands. This tool was also used to develop optimal VLS models for all four adenosine receptor subtypes [23], suggesting main structural determinants of subtype selectivity in this family. In prospective screening, the optimized A<sub>A2</sub>AR VLS model demonstrated an exceptionally high hit rate (40%), allowing discovery of a diverse and novel set of lead-like antagonists with as high as 60 nM affinity [21].

Note, that optimal VLS models may differ somewhat from individual ligand-receptor models – while the latter are optimized for binding of a specific ligand, the best VLS models represent a compromise between multiple ligand complexes. In some cases, different ligand-dependent receptor states can be clustered into two or more alternative VLS models, which can be used separately or in 4D screening procedures [66].

## Concluding remarks

Firmly grounded in high-resolution crystal structures of inactive GPCRs and supported by biochemical data, conformational modeling can be a practical tool helping to shape the emerging concept of activation mechanisms in adrenergic and potentially in other GPCRs. The modeling studies of agonist-GPCR complexes and later crystal structures have detailed small, but functionally important changes in the binding pocket allosterically coupled with larger downstream changes in the intracellular side of the receptor. Understanding of the remarkable diversity of ligand-dependent activation triggers can further benefit from comprehensive modeling of different ligand classes, which takes into account side chain and small backbone deviations in the binding pocket. As crystallography is yielding more structures of GPCRs, including first examples of active state GPCRs, this type of modeling will become even more accurate and reliable.

Although some important insight into agonists binding and induced changes can be gained without explicit modeling of downstream changes, understanding of GPCR signaling requires establishing the whole path from ligand binding to downstream activation of G-protein or other effectors. Recent crystal structures of the activated  $\beta_2$ AR- and  $A_{2A}$ AR-agonist complexes provide some details of such connections as a first step in establishing a reliable 3D framework for computational analysis of ligand structural and functional selectivity in these and other GPCRs.

Some other extensions of computational approaches may involve a combination of agonist modeling with GPCR subtype modeling [23] helping to generate a comprehensive picture of subtype and functional selectivity for whole GPCR subfamilies. Also, accumulation of experimental data on allosteric modulators and crystal structures of GPCRs may help to expand accurate conformational modeling to this important class of candidate drugs and their binding sites [67]. Of course in each case it will be vital to establish validation of the models through extensive ligand based benchmarking [21], biochemical studies and crystallography, when possible.

## Literature Cited

1. Tyndall JD, Sandilya R. GPCR agonists and antagonists in the clinic. *Med Chem.* 2005; 1(4):405–21. [PubMed: 16789897]
2. Overington JP, Al-Lazikani B, Hopkins AL. How many drug targets are there? *Nat Rev Drug Discov.* 2006; 5(12):993–6. [PubMed: 17139284]
3. Lagerstrom MC, Schiöth HB. Structural diversity of G protein-coupled receptors and significance for drug discovery. *Nat Rev Drug Discov.* 2008; 7(4):339–57. [PubMed: 18382464]
4. Smith NJ, Bennett KA, Milligan G. When simple agonism is not enough: emerging modalities of GPCR ligands. *Mol Cell Endocrinol.* 2011; 331(2):241–7. [PubMed: 20654693]
5. Cherezov V, et al. High-resolution crystal structure of an engineered human beta2-adrenergic G protein-coupled receptor. *Science.* 2007; 318(5854):1258–65. [PubMed: 17962520]
6. Rosenbaum DM, et al. GPCR engineering yields high-resolution structural insights into beta2-adrenergic receptor function. *Science.* 2007; 318(5854):1266–73. [PubMed: 17962519]
7. Warne T, et al. Structure of a beta(1)-adrenergic G-protein-coupled receptor. *Nature.* 2008; 454(7203):486–91. [PubMed: 18594507]
8. Wacker D, et al. Conserved binding mode of human beta2 adrenergic receptor inverse agonists and antagonist revealed by X-ray crystallography. *J Am Chem Soc.* 2010; 132(33):11443–5. [PubMed: 20669948]
9. Jaakola VP, et al. The 2.6 angstrom crystal structure of a human A2A adenosine receptor bound to an antagonist. *Science.* 2008; 322(5905):1211–7. [PubMed: 18832607]

10. Wu B, et al. Structures of the CXCR4 chemokine GPCR with small-molecule and cyclic peptide antagonists. *Science*. 2010; 330(6007):1066–71. [PubMed: 20929726]
11. Chien EY, et al. Structure of the human dopamine D3 receptor in complex with a D2/D3 selective antagonist. *Science*. 2010; 330(6007):1091–5. [PubMed: 21097933]
12. Shimamura T, et al. Molecular basis of antihistamine specificity against Human Histamine H1 receptor. *Nature*. 2011 accepted.
13. Reynolds, K.; Abagyan, R.; Katritch, V. Structure and Modeling of GPCRs: Implications for Drug Discovery. In: Gilchrist, A., editor. *GPCR Molecular Pharmacology and Drug Targeting: Shifting Paradigms and New Directions*. Wiley & Sons, Inc; Hoboken, NJ: 2010. p. 385-433.
14. Congreve M, et al. Progress in Structure Based Drug Design for G Protein-Coupled Receptors. *J Med Chem*. 2011
15. Topiol S, Sabio M. Use of the X-ray structure of the Beta2-adrenergic receptor for drug discovery. *Bioorg Med Chem Lett*. 2008; 18(5):1598–602. [PubMed: 18243704]
16. Reynolds KA, Katritch V, Abagyan R. Identifying conformational changes of the beta(2) adrenoceptor that enable accurate prediction of ligand/receptor interactions and screening for GPCR modulators. *J Comput Aided Mol Des*. 2009; 23(5):273–88. [PubMed: 19148767]
17. Katritch V, et al. Analysis of full and partial agonists binding to beta2-adrenergic receptor suggests a role of transmembrane helix V in agonist-specific conformational changes. *J Mol Recognit*. 2009; 22(4):307–18. [PubMed: 19353579]
18. Jaakola VP, et al. Ligand binding and subtype selectivity of the human A(2A) adenosine receptor: identification and characterization of essential amino acid residues. *J Biol Chem*. 2010; 285(17): 13032–44. [PubMed: 20147292]
19. Sabio M, Jones K, Topiol S. Use of the X-ray structure of the beta2-adrenergic receptor for drug discovery. Part 2: Identification of active compounds. *Bioorg Med Chem Lett*. 2008; 18(20):5391–5. [PubMed: 18829308]
20. Kolb P, et al. Structure-based discovery of {beta}2-adrenergic receptor ligands. *Proc Natl Acad Sci U S A*. 2009
21. Katritch V, et al. Structure-based discovery of novel chemotypes for adenosine A(2A) receptor antagonists. *J Med Chem*. 2010; 53(4):1799–809. [PubMed: 20095623]
22. Carlsson J, et al. Structure-Based Discovery of A(2A) Adenosine Receptor Ligands. *J Med Chem*. 2010
23. Katritch V, Kufareva I, Abagyan R. Structure based prediction of subtype-selectivity for adenosine receptor antagonists. *Neuropharmacology*. 2011; 60(1):108–15. [PubMed: 20637786]
24. Kobilka B, Schertler GF. New G-protein-coupled receptor crystal structures: insights and limitations. *Trends Pharmacol Sci*. 2008
25. Altenbach C, et al. High-resolution distance mapping in rhodopsin reveals the pattern of helix movement due to activation. *Proc Natl Acad Sci U S A*. 2008; 105(21):7439–44. [PubMed: 18490656]
26. Scheerer P, et al. Crystal structure of opsin in its G-protein-interacting conformation. *Nature*. 2008; 455(7212):497–502. [PubMed: 18818650]
27. Schwartz TW, et al. Molecular mechanism of 7TM receptor activation--a global toggle switch model. *Annu Rev Pharmacol Toxicol*. 2006; 46:481–519. [PubMed: 16402913]
28. de Graaf C, Rognan D. Selective structure-based virtual screening for full and partial agonists of the beta2 adrenergic receptor. *J Med Chem*. 2008; 51(16):4978–85. [PubMed: 18680279]
29. Ivanov AA, Barak D, Jacobson KA. Evaluation of Homology Modeling of G-Protein-Coupled Receptors in Light of the A(2A) Adenosine Receptor Crystallographic Structure. *J Med Chem*. 2009
30. Rasmussen SG, et al. Structure of a nanobody-stabilized active state of the beta(2) adrenoceptor. *Nature*. 2011; 469(7329):175–80. [PubMed: 21228869]
31. Rosenbaum DM, et al. Structure and function of an irreversible agonist-beta(2) adrenoceptor complex. *Nature*. 2011; 469(7329):236–40. [PubMed: 21228876]
32. Warne T, et al. The structural basis for agonist and partial agonist action on a beta(1)-adrenergic receptor. *Nature*. 2011; 469(7329):241–4. [PubMed: 21228877]



33. Xu F, et al. Structure of an Agonist-Bound Human A2A Adenosine Receptor. *Science*. 2011; 332(6027):322–327. [PubMed: 21393508]
34. Lebon G, et al. Agonist-bound adenosine A(2A) receptor structures reveal common features of GPCR activation. *Nature*. 2011
35. Strader CD, et al. Conserved aspartic acid residues 79 and 113 of the beta-adrenergic receptor have different roles in receptor function. *J Biol Chem*. 1988; 263(21):10267–71. [PubMed: 2899076]
36. Strader CD, et al. Identification of two serine residues involved in agonist activation of the beta-adrenergic receptor. *J Biol Chem*. 1989; 264(23):13572–8. [PubMed: 2547766]
37. Liapakis G, et al. The forgotten serine. A critical role for Ser-2035.42 in ligand binding to and activation of the beta 2-adrenergic receptor. *J Biol Chem*. 2000; 275(48):37779–88. [PubMed: 10964911]
38. Shi L, et al. Beta2 adrenergic receptor activation. Modulation of the proline kink in transmembrane 6 by a rotamer toggle switch. *J Biol Chem*. 2002; 277(43):40989–96. [PubMed: 12167654]
39. Wieland K, et al. Involvement of Asn-293 in stereospecific agonist recognition and in activation of the beta 2-adrenergic receptor. *Proc Natl Acad Sci U S A*. 1996; 93(17):9276–81. [PubMed: 8799191]
40. Kobilka BK. G protein coupled receptor structure and activation. *Biochim Biophys Acta*. 2007; 1768(4):794–807. [PubMed: 17188232]
41. Nygaard R, et al. Ligand binding and micro-switches in 7TM receptor structures. *Trends Pharmacol Sci*. 2009; 30(5):249–59. [PubMed: 19375807]
42. Simpson LM, et al. Modeling GPCR active state conformations: the beta(2)-adrenergic receptor. *Proteins*. 2011; 79(5):1441–57. [PubMed: 21337626]
43. Vanni S, et al. Predicting novel binding modes of agonists to beta adrenergic receptors using all-atom molecular dynamics simulations. *PLoS Comput Biol*. 2011; 7(1):e1001053. [PubMed: 21253557]
44. Bhattacharya S, et al. Ligand-stabilized conformational states of human beta(2) adrenergic receptor: insight into G-protein-coupled receptor activation. *Biophys J*. 2008; 94(6):2027–42. [PubMed: 18065472]
45. Pooput C, et al. Structural basis of the selectivity of the beta(2)-adrenergic receptor for fluorinated catecholamines. *Bioorg Med Chem*. 2009; 17(23):7987–92. [PubMed: 19857969]
46. Totrov M, Abagyan R. Flexible protein-ligand docking by global energy optimization in internal coordinates. *Proteins*. 1997; Suppl 1:215–20. [PubMed: 9485515]
47. Abagyan, RA., et al. ICM Manual. MolSoft LLC; La Jolla, CA: 2011.
48. Abagyan R, Totrov M. Biased probability Monte Carlo conformational searches and electrostatic calculations for peptides and proteins. *J Mol Biol*. 1994; 235(3):983–1002. [PubMed: 8289329]
49. Abagyan RA, Totrov MM, Kuznetsov DA. Icm: A New Method For Protein Modeling and Design: Applications To Docking and Structure Prediction From The Distorted Native Conformation. *J Comp Chem*. 1994; 15:488–506.
50. Vilar S, et al. In silico analysis of the binding of agonists and blockers to the beta2-adrenergic receptor. *J Mol Graph Model*. 2011; 29(6):809–17. [PubMed: 21334234]
51. Ambrosio C, et al. Catechol-binding serines of beta(2)-adrenergic receptors control the equilibrium between active and inactive receptor states. *Mol Pharmacol*. 2000; 57(1):198–210. [PubMed: 10617695]
52. Liapakis G, et al. Synergistic contributions of the functional groups of epinephrine to its affinity and efficacy at the beta2 adrenergic receptor. *Mol Pharmacol*. 2004; 65(5):1181–90. [PubMed: 15102946]
53. Sato T, et al. Ser203 as well as Ser204 and Ser207 in fifth transmembrane domain of the human beta2-adrenoceptor contributes to agonist binding and receptor activation. *Br J Pharmacol*. 1999; 128(2):272–4. [PubMed: 10510435]
54. Hannawacker A, Krasel C, Lohse MJ. Mutation of Asn293 to Asp in transmembrane helix VI abolishes agonist-induced but not constitutive activity of the beta(2)-adrenergic receptor. *Mol Pharmacol*. 2002; 62(6):1431–7. [PubMed: 12435811]

55. Xhaard H, et al. Molecular evolution of adrenoceptors and dopamine receptors: implications for the binding of catecholamines. *J Med Chem.* 2006; 49(5):1706–19. [PubMed: 16509586]
56. Kufareva I, et al. Status of GPCR modeling and docking as reflected by community wide GPCR Dock 2010 assessment. *Structure.* 2011 accepted.
57. Dror RO, et al. Identification of two distinct inactive conformations of the beta2-adrenergic receptor reconciles structural and biochemical observations. *Proc Natl Acad Sci U S A.* 2009; 106(12):4689–94. [PubMed: 19258456]
58. Park JH, et al. Crystal structure of the ligand-free G-protein-coupled receptor opsin. *Nature.* 2008
59. Standfuss J, et al. The structural basis of agonist-induced activation in constitutively active rhodopsin. *Nature.* 2011; 471(7340):656–60. [PubMed: 21389983]
60. Rasmussen SG, et al. Crystal structure of the beta(2) adrenergic receptor-Gs protein complex. *Nature.* 2011
61. Changeux JP, Edelstein SJ. Allosteric mechanisms of signal transduction. *Science.* 2005; 308(5727):1424–8. [PubMed: 15933191]
62. Kenakin T, Miller LJ. Seven transmembrane receptors as shapeshifting proteins: the impact of allosteric modulation and functional selectivity on new drug discovery. *Pharmacol Rev.* 2010; 62(2):265–304. [PubMed: 20392808]
63. Warne T, et al. Development and crystallization of a minimal thermostabilised G protein-coupled receptor. *Protein Expr Purif.* 2009; 65(2):204–13. [PubMed: 19297694]
64. Katritch V, et al. GPCR 3D homology models for ligand screening: lessons learned from blind predictions of adenosine A2a receptor complex. *Proteins.* 2010; 78(1):197–211. [PubMed: 20063437]
65. Katritch, V.; Rueda, M.; Abagyan, R. Ligand Guided Receptor Optimization. In: Orry, A.; Abagyan, R., editors. *Homology Modeling.* Springer; 2011. in press
66. Bottegoni G, et al. Four-dimensional docking: a fast and accurate account of discrete receptor flexibility in ligand docking. *J Med Chem.* 2009; 52(2):397–406. [PubMed: 19090659]
67. Keov P, Sexton PM, Christopoulos A. Allosteric modulation of G protein-coupled receptors: a pharmacological perspective. *Neuropharmacology.* 2011; 60(1):24–35. [PubMed: 20637785]

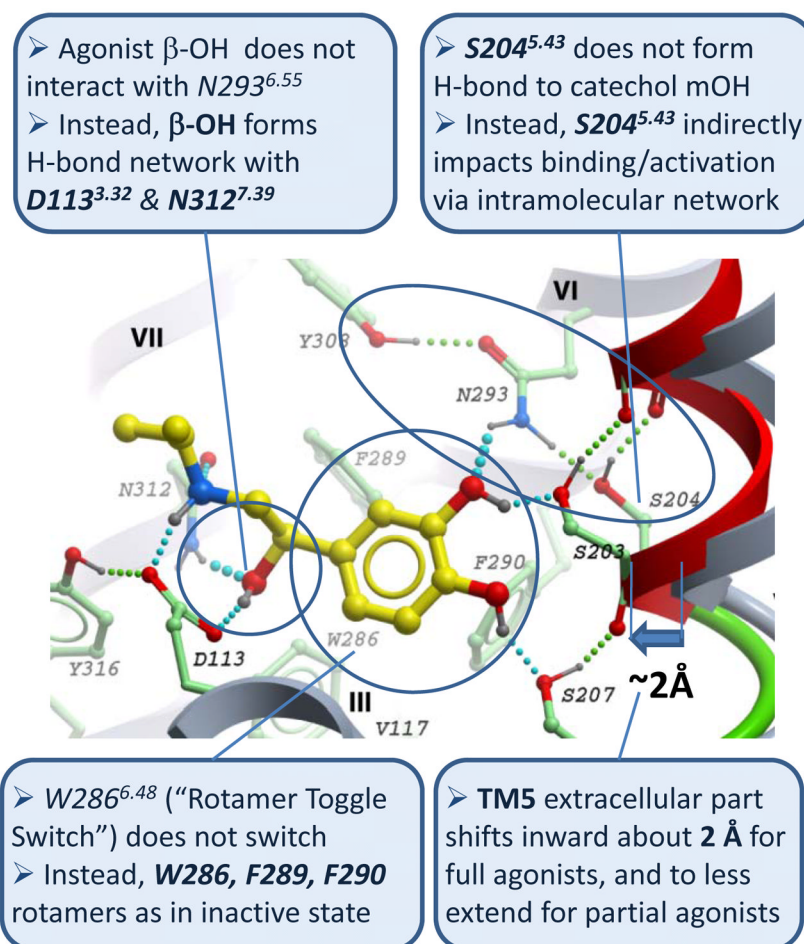


**Figure 1.** Key new features of full agonist isoproterenol binding and conformational changes in  $\beta_2$ AR ligand binding pocket predicted in 2008 by conformational modeling based on crystal structure of inactive structure of the  $\beta_2$ AR-carazolol complex (PDB:2rh1). In this published model (see Supplementary Info in ref. [17]) ligand is shown with yellow carbons, while the contact residues of the  $\beta_2$ AR shown with green carbons. Shifted TM5 helix (red and green ribbon) is compared to the original backbone in the crystal structure. Predicted hydrogen bonds are shown by cyan (ligand-receptor) and green (intramolecular) spheres.

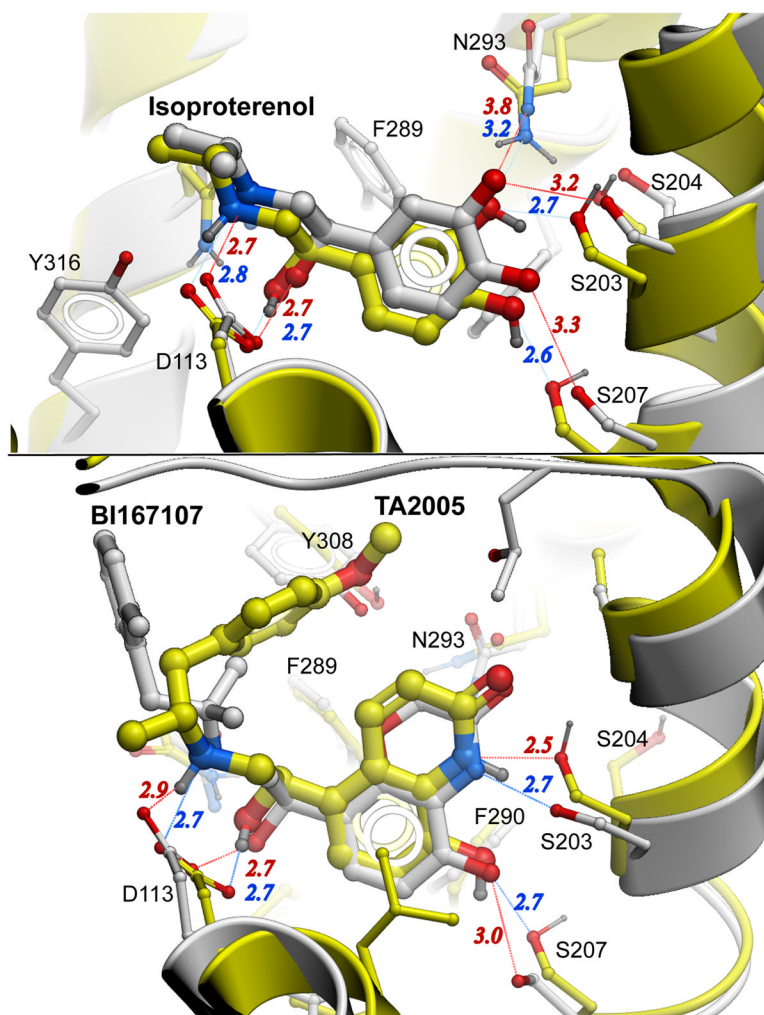


**Figure 2.**

Accuracy of agonist  $\beta_2$ AR binding predictions. Predicted in ref [17] models are shown with yellow carbons and blue polar interaction distances, while crystal structures are shown with grey carbon atoms and red interaction distances. (A) Comparison of agonist-receptor interactions in the energy-optimized Isoproterenol- $\beta_2$ AR model and the crystal structure of Isoproterenol complex with the closely related  $\beta_1$ AR (PDB: 2Y03), which has identical residues of the binding pocket. The model correctly predicted all ligand-receptor polar interactions and hydrophobic contacts (100 % identical contacts at 4 Å cutoff). Agonist poses have Rmsd = 0.8 Å, while contact side chains Rmsd = 1.1 Å between predicted and crystal structure. Note that in the crystal structure the  $\beta_1$ AR is in inactive state, with hydrogen bonds still having slightly suboptimal length. Further minor inward adjustment of TM5 position and a corresponding slight shift of ligand that are likely to occur upon activation of the receptor should improve model/structure RMSD even further. (B) Comparison of ligand-receptor interactions between the energy-optimized model of TA2005- $\beta_2$ AR and the crystal structure of the BI-167107- $\beta_2$ AR complex in nanobody-stabilized active state. Similar aromatic and ethanolamine moieties of these full agonists have RMSD=0.5 Å, and binding pocket contact side chains RMSD=0.9 Å. The phenol containing “tail” of BI-167107 does not have polar groups as in TA2005, which may explain differences in this part of the complex.

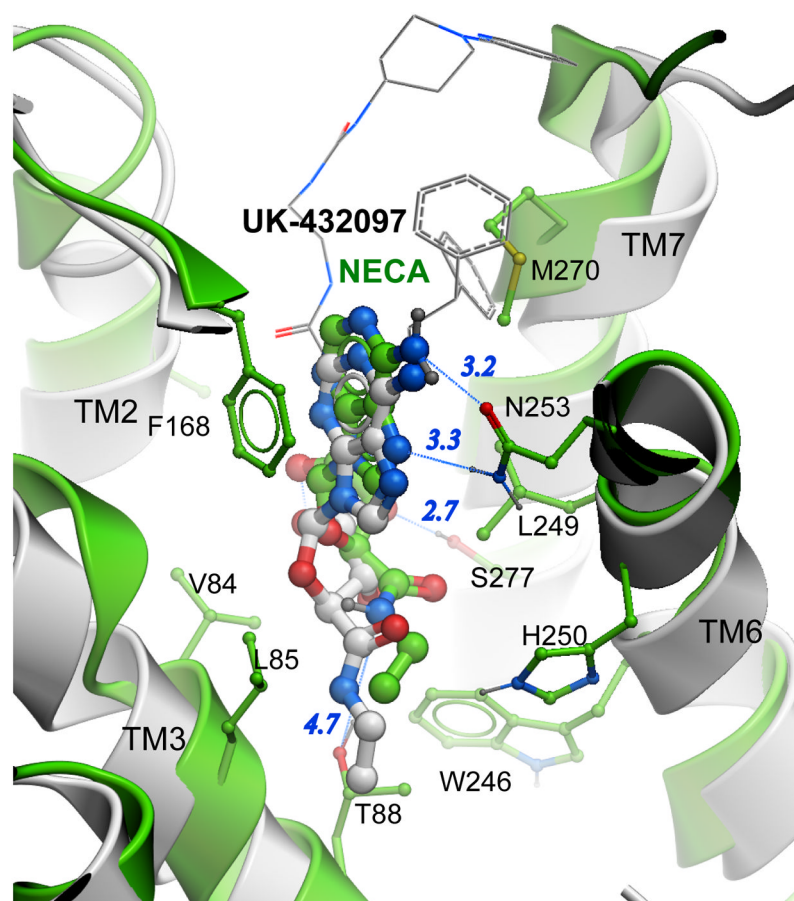


**Figure 3.** Adenosine  $A_{2A}$  receptor agonist binding. Predicted in ref [18] model of the NECA- $A_{2A}$ AR complex is shown with green carbons, while the UK-432097 agonist and protein backbone of crystal structure [33] (PDB: 3QAK) are shown with grey. For clarity, bulky C2 and N6 substitutions UK-432097 are shown by thin lines. Key polar interactions are shown by blue lines and distances in Angstroms. Comparison of common substructures of two agonists shows predictions of NECA binding pose with RMSD 1.7 Å, which reproduces most polar interactions for the agonists ribose ring. At the same time, the NECA molecule in the model is systematically shifted upwards, which precludes optimal interaction of its amide group with the Thr88<sup>3,36</sup> side chain. Adjustment of the ligand into its optimal position and engagement of all polar interactions requires a shift of the conserved Trp246<sup>6,48</sup> side chain, which is a part of activation mechanism in the  $A_{2A}$ AR and some other GPCRs.